D3.5
Methodology for signal processing assessment agreed

General information	
Grant agreement number	755500
Start date of the project	01/09/2017
Project duration	48 months
Due date of the deliverable	28/02/2019
Actual submission date	14/10/2020
Lead beneficiary	9 – KTU

Keywords
Methodology, signal processing, survey

Type	Meaning	
R	Document, report	x
DEM	Demonstrator, pilot, prototype	
DEC	Websites, patent fillings, videos, etc.	
OTHER	Software, technical diagram, etc.	

Dissemination Level		
PU	Public	x
CO	Confidential, only for members of the consortium (including the Commission Services)	

Table of Contents

Table of Figures

Table of Tables

Glossary

Abbreviations/Acronym	Description
DORT	Decomposition of the Time Reversal Operator
FBH	Flat bottom hole
FMC	Full matrix capture
MSF-DORT	Multiple Scattering Filter DORT
PWE	Plane wave excitation
PWI	Plane wave imaging
SAFT	Synthetic Aperture Focusing Technique
SDH	Side drilled hole
TFM	Total focusing method
TRL	Transmit-receive longitudinal

1 Summary

This report is dedicated to the WP3. The aim of this document is to introduce the proposed methodology for assessment of imaging algorithms. The main objective of the proposed methodology is to quantify the improvements of imaging algorithm performance achieved throughout the Advise project. In order to create methodology, the survey with the appropriate questions was created by KTU with support of EDF and Framatome. The questionnaire consists of 32 questions, grouped into four categories: samples, targeted defects, imaging algorithms and assessment procedure. The questionnaire was distributed among project partners. Totally 13 answers have been obtained from 9 different institutions. The answers enabled to identify mock-ups, reference imaging techniques and comparison metrics that will be used for imaging algorithm assessement. Based on the survey, the methodology was prepared and presented as the deliverable D3.5.

2 Introduction

The complex and heterogeneous structures, in particular coarse grained materials, castings and austenitic welds commonly found in nuclear installations significantly degrade the performance of ultrasonic inspection techniques. This is due to microstructures with large grains, inducing scattering of the ultrasonic waves at grain boundaries, which is responsible for both structural noise and attenuation. The ADVISE project WP3 seeks to enhance and optimise currently available inspection strategies for challenging materials, specifically for coarse-grained metals and research novel inspection alternatives. Therefore the project focuses on imaging and signal processing methods that can show demonstrable signal to noise improvements on coarse-grained metals, which lead to the enchancing of quality of an ultrasonic image.

As a result, implementation and extension of different imaging methods, such as TFM, SAFT, MSF-DORT, frequency and spatial compounding, which have widespread scientific uptake, but not investigated enough for the coarse-grained materials are of particular interest. As many different imaging techniques are being developed by the ADVISE project, each having their own benefits, a strict and unified way to quantify the improvement of extended algorithms over the classical ones is required. Hence, the aim of this deliverable is to propose and describe a methodology, which offers a guidelines for comparison between classical and extended imaging algorithms. It's expected, that proposed metholodogy will allow to explore potential of each extended imaging algorithm and will enable them to be better applied to coarse-grained sample inspection. For this purpose the questionnaire dedicated to imaging algorithm assessment methodology was prepared and distributed among the partners of the consortium. Totally 13 responses have been obtained from 9 different institutions, which formed a basis for definition of the methodology. Based on the results of the survey, a methodology has been proposed.

The prepared methodology is a guideline for the ADVISE partners to quantify improvement of imaging algorithm performance achieved throughout the project. It contains a detailed description of the mock-ups, data acquisition set-ups and comparison metrics of imaging techniques. A special study was prepared on signal to noise (SNR) and contrast to noise ratio (CNR) evaluation to raise the awareness of different means of SNR and CNR calculation, their advantages and shortcommings.

As a result, such methodology brings a unified way to assess the imaging algorithms and to emphasize their benefits over existing techniques in terms of inspection of coarse-grained metals. In the few upcoming chapters, the answers obtained from project partners will be revised followed by the proposed methodology.

3 Description of the questionnaire

The proposed survey contains 32 questions, arranged into four groups: samples, targeted defects, imaging algorithms and assessment procedure. Each group has specific questions related to the topic, in order to idenfiy suitable mock-ups, data acquisition techniques and parameters that will be used to quantify imaging methods. The questionnairre was adjusted to the expertise of each partner of the project, allowing them to skip some of the questions. Totally, 13 answers from the respondents were colleted. The participants of the survey are presented in Table 3.1. The questionnaire is presented in Annex 1.

Table 3.1: Participants of the survey

Partner institution	EDF	ICL	Fraunhofer	CEA	UoB	M2M	BZN	Framatome	UJV
No. of participants	1	1	2	1	2	2	1	2	1

3.1 Samples and targeted defects

The part of the questionnaire related to samples and targeted defects had the goal to select the appropriate samples for assessment of imaging algorithm developed under the project and to identify the defects needs to be detected. The main set of characteristics, which must be evaluated are: geometry and material of the sample; type, size and position of the defect; the position or side from which the defect should be inspected and detected. The samples were selected from the list of R&D mock-ups, provided by project partners. The samples, proposed by respondents, can be divided into 2 main groups: **welds** (weld repair and V-shape weld) and **cast/ coarse-grained** (coarse grained and static cast stainless steel) components. The samples most frequently selected by partners are:

- 1774-T248A – 9 respondents;
- 1517-T105EE-2G-GA – 8 respondents;
- D522-TG – 9 respondents;
- 1618-B359-B1 – 9 respondents.

The **1618-B359-B1** is a nickel based alloy (Inconel 600) mock-up, that has average grain size of 90 µm. **D522-TG** is a coarse grained stainless steel, cast autenoferritic mock-up. **1517-T105EE-2G-GA** is a U chamfer, shielded metal manual arc weld with 30 welding passes. It possesses no disorientation in the welding direction and high disorientation of the average grain tilt. Finally, **1774-T248A** is a weld cladding repair mock-up, made from Ni based alloy. It has homogeneous microstructure and quasi-vertical grains. Slight grain disorientation is observed at chamfers.

The majority of respondents decided that the expected grain size ranges for imaging algorithm verification should be between 50µm and 800µm. The proposed samples represent the following components and materials: cast stainless steel based alloys; V-shaped welds; weld repairs and cast Ni based alloys. Among the samples selected above, one of them (**1618-B359-B1**) has been characterised metallograhically, while the others expected to have average grains in the desired range (50µm–800µm).

The most expected types of defects between the respondents are presented in Fig. 3.1. The nature of the defects under investigation should be both artificial and natural (8 resp.), or artificial only (5 resp.). The majority of respondents appreciate these defect types: SDH (13 resp.), notches (13 resp.), FBH (6 resp.) in case of artificial defects and cracks (13 resp.) in case of natural origin defects. All the samples listed above has artificial defects with known positions and sizes.

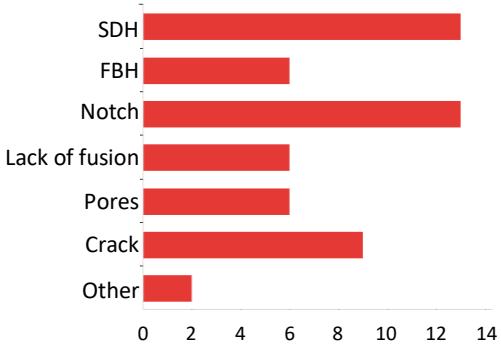

Figure 3.1: Expected types of the defects (responses of the partners)

In the case of weld repair (**1774-T248A**) and thin welds (**1517-T105EE-2G-GA**) the appropriate defects are SDH and notches. In the case of cast/coarse-grained steel (**1618-B359-B1**, **D522-TG**) defect types are SDH and FBH. The size ranges for natural and artificial defects established on the bases on the received responses are summarized in Table 3.2.

Table 3.2: Parameters of the defects (based on responses)

Nature of the defect	Defect type	Parameters of the defect	Location
Natural	Crack	Length 1-20 mm ; Height 2-6 mm	Surface breaking
Artificial	Notches	Length 10 mm ; Depth 10-20 mm	Middle, bottom
	SDH	Size 2-5 mm Depth 10-20 mm *d* = 2 mm	Middle, bottom
	FBH	*d* = 3 mm	Middle

All selected samples (**1774-T248A**, **D522-TG**, **1517-T105EE-2G-GA** and **1618-B359-B1**) meet the required parameters for defect size, presented in the table above. The **1618-B359-B1** has 4 side-drilled holes (SDH) (*d* = 2mm) located at depths 10mm, 30mm, 50mm, 70mm and 2 flat-bottom holes (FBH) (*d* = 4mm and 8mm) situated at bottom of the mock-up. **D522-TG** possess 5 SDH (*d* = 0.5 mm) and 5 SDH (*d* = 1mm), that are located close to surface of the sample at depths in range of 5mm to 30mm. Thin weld sample **1517-T105EE-2G-GA** has 2 SDH (*d* = 1.5 mm) that are located the middle of the weld at depths of 10mm and 20mm. Finally, **1774-T248A** has 4 SDH (*d* = 2 mm at depths of 9mm and 15mm), 4 vertical notches and 5 tilted notches. Two notches, one from each group has an opening angle of 3.2°. All notches are surface breaking defects, with the heights in the range from 5mm to 28mm.

The respondents noted that the dimensions of the targeted defects should be known in advance in order to quantify assessment of the imaging algorithm in the case of machined defects, but not necessarily in case of natural origin defects. So called “blind” experiments, without initial knowledge about defects, would be useful just on a final qualification phase of the imaging algorithm.

3.2 Imaging algorithms

The aim of this part of questionnaire was to identify data acquisition set-ups, reference imaging techniques and assessment parameters for quantification of newly proposed algorithm. The same set-ups should be used for reference imaging techniques and the ones proposed throughout “Advise” project. In all cases measurements are performed by using phased array techniques. According to the samples under investigation, several measurement set-ups are appreciated between the partners: contact, wedge and TRL. The majority of respondents appreciate angle beam measurement set-up with wedge (5 resp.) and TRL (3 resp.) for the coarse grained stainless steel mock-up **D522-TG**. The proposed data acquisition methods in this case are FMC (4 resp.) and PWE (3 resp.).

For the case of the nickel based alloy (Inconel 600) mock-up **1618-B359-B1** most of respondents (6 resp.) noticed the direct contact method as more suitable. The appreciated data acquisition methods are FMC (7 resp.) and PWE (4 resp.)

The majority of respondents noticed that contact measurement method without wedge (7 resp.) and TRL (3 resp.) are more appropriate for the sample **1517-T105EE-2G-GA** (shielded metal). The data acquisition methods are FMC (7 resp.) and PWE (4 resp.).

Weld cladding repair mock-up **1774-T248A** should be investigated by phased array with wedge (7 resp.) and TRL (4 resp.). The dominant data acquisition method in this case is FMC (9 resp.). The parameters of the appreciated inspection techniques (frequency, angle, scaning type, position of the array) are selected personally by the partners. It depends on sample under investigation (weld, cast, coarse grained and etc.) and positions of defects. It was identified that the parameters, which should be used for quantification of imaging algorithm are (Fig. 3.2):

- detectability of defects (12 resp.);
- defect sizing (11 resp.);
- defect positioning (10 resp.);
- SNR (8 resp.);
- coverage area (7 resp.).

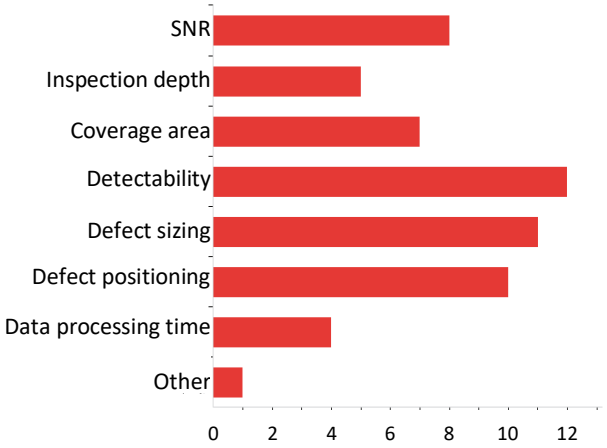

Figure 3.2: Quantification metrics for imaging algorithm assessment (responses of the partners)

These parameters will be used to evaluate the performance of newly proposed imaging techniques. The same metrics will be applied to reference imaging method (TFM) and to the technique under quantification.

3.3 Assessment procedure

The objective of this part of the questionnaire was to identify the expected improvement of newly proposed imaging algorithms. The main parameters, which were needed to quantify are: SNR, inspection depth, detectability and defect sizing.

The majority of respondents identified that expected improvement in terms of SNR are 20-30% according to the reference. The improvement in terms of inspection depth depends on sample under investigation. The capability to inspect the first 30 mm of a cast/coarse-grained components are appreciated by most respondents (7 resp.). Inspection depth of 60 mm should be achieved in the case of weld repair and v-shape welds (7resp.). The responses related to detectability of defects are very scattered. Expected improvement is either 10-20% (3 resp.) or 20-30% (4 resp.). The results for defect detectability are presented in Fig. 3.3 (a). In case of defect sizing, the majority of respondents expect about 20-30% of defect size estimation imporvement (4 resp.), 2 respondents expect 10-20% (2 resp.), while other partners have no strict opinion about that. The results for defect sizing are presented in Fig. 3.3(b).

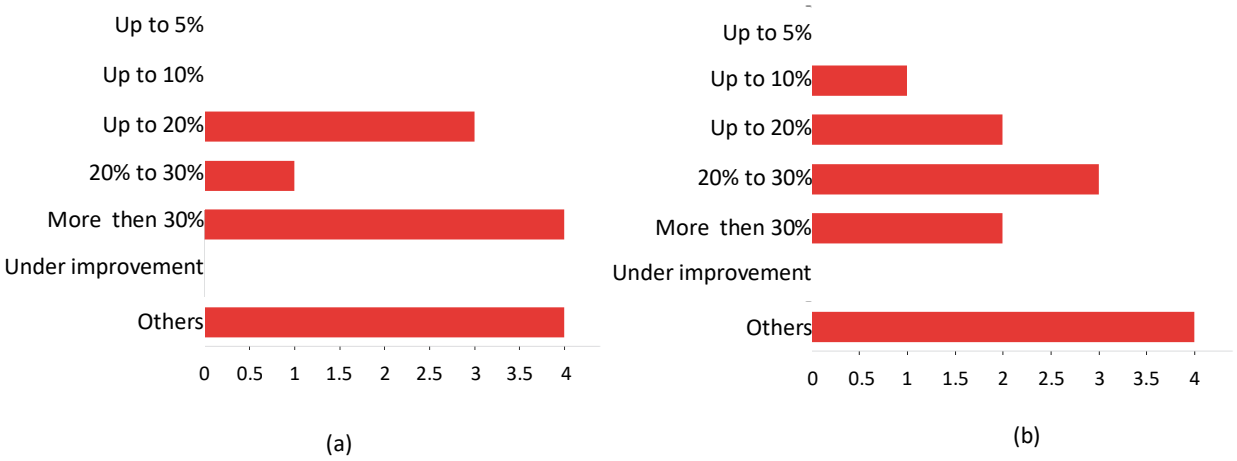

Figure 3.3: Expected improvement of defect detectability (a) and sizing (b) (responses of the partners)

Another important aspect was to identify the targeted sensitivity of the imaging algorithm in general. According to the survey, for the frequency range 1-5 MHz the sensitivity 0.3-0.5 mm is expected. In case of TFM image, the sensitivity of the order of wavelength/5 is appreciated. Please note that sensitivity in this case means the ability to locate smallest possible discontinuities at a given frequency.

In order to make verification and quantification of the imaging algorithm performance and to make the comparison of newly proposed imaging algorithms, the reference inspection method, so called "gold standard", must be identified. Based on received answers (Fig. 3.4), TFM method may be used as a reference imaging technique (4 resp.). Depending on the sample and inspection set-up, the combination of TRL data acquisition and TFM reconstruction method can be used as a reference (3 resp.). In other cases, where the contact techniques are enough, classical TFM shall be used.

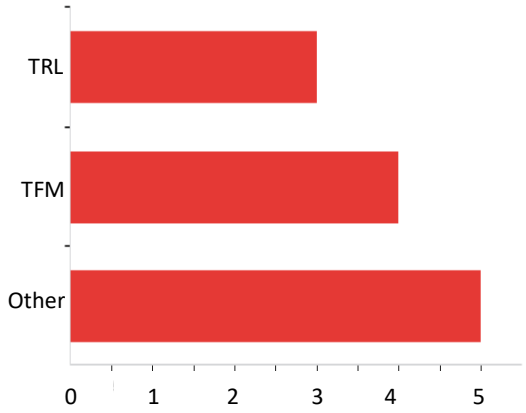

Figure 3.4: Reference inspection methods (responses of the partners)

The involvement of the project partners in the assessment of imaging algorithms was identified as well. The partners from EDF, Framatome and KTU are will be responsible for the samples and defects selection, preparation and process coordination. Framatome, CEA and KTU will take a role in the implementation of the TRL and TFM reference techniques on the selected samples. M2M, CEA and UoB will be involved in testing of newly proposed imaging techniques. KTU can assess the parameters of the artificial defects by conventional NDT techniques if neccesarry. The prepared methodology is presented in Annex 2.

4 Conclusion

The questionnaire to identify mock-ups, inspection set-ups, reference imaging techniques and quantification parameters has been created, in order to prepare the methodology for assessment of newly proposed imaging algorithms. Four different samples in two groups (cast components and welds) were identified as most suitable for the assessment, considering grain size ranges and the expected artificial defect types defined by the respondents. Three different data acquisition set-ups (FMC, TRL and PWE) were distinguished for collection of the signals from the identified mock-ups. The total focussing method has been identified as a reference method and will be used in comparison with the newly proposed imaging techniques. The reference and proposed methods will be compared by five different parameters (detectability, inspection depth, SNR, defect sizing and positioning) in order to quantify the achieved improvement. As a result of the questionnaire, the methodology for assessment of imaging techniques has been created. The unified methodology will enable to carry out the inspection of the same samples using slightly different imaging algorithms or even new approaches of signal processing . The acquired inspection data will be shared between partners and processed using different algorithms and codes. Comparison of the processing methods and imaging techniques will lead to the selection of most accurate, most efficient and most practical techniques for different cases of coarse-grained materials and components.

5 Annex 1

Advise D3.5 questionnaire

Survey Flow

Intro
SAMPLES (5 Questions)
TARGETED DEFECTS (9 Questions)
IMAGING ALGORITHMS (5 Questions)
ASSESSMENT PROCEDURE (11 Questions)
Summary (2 Questions)

Start of Block: Intro

This questionnaire is dedicated to imaging algorithm assessment methodology. Based on the received answers, the deliverable D3.5 and the guidelines will be prepared that will quantify improvement of imaging algorithm performance achieved throughout the Advise project. The questions are arranged in 4 groups according to the topics: samples, defects, imaging algorithms and assessment procedure. The survey contains 32 questions while the estimated duration is 8 minutes.

End of Block: Intro

Start of Block: SAMPLES

SAMPLES: Object of inspection and reference samples (geometries, structure, grain size, inspection positions etc.);

Q1 Which samples from the mock-up list appear most suited for imaging algorithm assessment? Refer to specific samples. [link to the mock-up list]

- ○ 1. Reference code of mock-up no. 1 (1) _____
- ○ 2. Reference code of mock-up no. 2 (2) _____
- ○ 3. Reference code of mock-up no. 3 (3) _____
- ○ 4. Reference code of mock-up no. 4 (4) _____
- ○ 5. Reference code of mock-up no. 5 (5) _____

Q2 Do you think it is relevant to prepare special samples for imaging algorithm verification?

- ○ Yes (1)
- ○ No (2)

○ Other (please specify) (3) _____

Q3 What grain size ranges are expected for imaging algorithm verification task?

- ☐ 50µm-250µm (grain index 6 to 1) (1)
- ☐ 250µm-500µm (grain index : 1 to -1) (2)
- ☐ 500µm-1000µm (grain index : -1 to -3) (3)
- ☐ 1000µm+ (grain index : less than -3) (4)

Q4 Which components are of interest?

- ☐ Cast Ni based alloys (1)
- ☐ Cast stainless steel based alloys (2)
- ☐ Weld molds (3)
- ☐ V-shaped welds (4)
- ☐ K-shaped welds (5)
- ☐ Weld repairs (6)
- ☐ Dissimilar Metal Welds (DMW) (7)
- ☐ Narrow Gap welds (8)
- ☐ Cladded welds (9)
- ☐ Other components (please specify type and thickness) (10) _____

Q5 Which inspection set-ups are of interest for assessment of imaging algorithms?

	Contact (1)	Wedge (2)	Immersion (3)	TRL (4)
Mock-up no. 1 (1)	○	○	○	○
Mock-up no. 2 (2)	○	○	○	○
Mock-up no. 3 (3)	○	○	○	○
Mock-up no. 4 (4)	○	○	○	○
Mock-up no. 5 (5)	○	○	○	○

End of Block: SAMPLES

Start of Block: TARGETED DEFECTS

TARGETED DEFECTS: Defects to be detected and their parameters (type, size, orientation, positions etc.);

Q6 What type of defects are relevant for phased array imaging algorithm verification purposes?

- ☐ Side drilled hole (SDH) (1)
- ☐ Flat bottom hole (FBH) (2)
- ☐ Notch (3)
- ☐ Lack of fusion (4)
- ☐ Pores (5)
- ☐ Cracks (6)
- ☐ Other (please specify) (7) _____

Q7 What should be the nature of targeted defects?

- ○ Natural in service defects (1)
- ○ Natural manufacturing defects (4)
- ○ Artificial (2)
- ○ Both (3)

Q8 What are relevant size ranges (length and height) of targeted defects?

- ○ Natural origin defect sizes (1) _____
- ○ Artificial defect sizes (2) _____
- ○ Other (please specify) (3) _____

Q9 What are locations of targeted defects (surface breaking, subsurface, middle, bottom)?

- ○ Relevant locations for cast components (please specify) (1) _____
- ○ Relevant locations for welds (please specify) (2) _____
- ○ Other (please specify) (3) _____

Q10 What are researched characteristics of defects?

- ☐ Detection only (1)
- ☐ Amplitude related to a reference reflector (2)
- ☐ Characteristic of the defect (volumic or non volumic) (3)
- ☐ Location (depth Z, positions X, Y) (4)
- ☐ Length (5)
- ☐ Height (6)
- ☐ Single defect or cluster of defects (7)
- ☐ Other (please specify) (8) _____

Q11 Are there any “blind” experiments required for algorithm assessment without initial knowledge about defects?

- ○ Yes (1)
- ○ No (2)
- ○ Other (please specify) (3) _____

Q12 Does the assessment of defect require manual defect classification by the operator? (in case of natural origin defects)

- ○ Yes (1)
- ○ No (2)
- ○ Other (please specify) (3) _____

Q13 How the defect parameters (length, depth, height) will be quantified?

- ○ Manual mechanical measurement (for artificial defects) (1)
- ○ Assessment using conventional NDT methods (2)
- ○ Both (3)
- ○ Other (please specify) (4) _____

Q14 Are the dimensions of the targeted defects known in order quantify assessment of the imaging algorithms?

- ○ Yes (1)
- ○ No (2)
- ○ Has to be determined by an expert (3)
- ○ Other (please specify) (4) _____

End of Block: TARGETED DEFECTS

Start of Block: IMAGING ALGORITHMS

IMAGING ALGORITHMS: Inspection techniques to be used and techniques for comparison (phased array, beamforming, TOFD etc.);

Q15 Which parameters should be used to quantify the improvement of imaging algorithms?

- ☐ SNR (1)
- ☐ Inspection depth (7)
- ☐ Coverage area (8)
- ☐ Detecteability of defects (2)
- ☐ Defect sizing (3)

- [ ] Defect positioning (4)
- [ ] Data processing time (5)
- [ ] Other (please specify) (6) _____

Q16 Which particular imaging algorithms (i.e. TFM, SAFT, DORT, HMC, PWI, VSA) are of interest for testing (taking into the account selected mock-ups)?

- ○ 1. Mock-up no. 1 (1) _____
- ○ 2. Mock-up no. 2 (2) _____
- ○ 3. Mock-up no. 3 (3) _____
- ○ 4. Mock-up no. 4 (4) _____
- ○ 5. Mock-up no. 5 (5) _____

Q17 Which beam formation and data acquisition set-ups shall be used for imaging algorithm verification? Relate the beam formation/data acquisition set-up to specific samples.

	Mock-up no. 1 (1)	Mock-up no. 2 (2)	Mock-up no. 3 (3)	Mock-up no. 4 (4)	Mock-up no. 5 (5)
FMC (1)	☐	☐	☐	☐	☐
HMC (2)	☐	☐	☐	☐	☐
TFM (3)	☐	☐	☐	☐	☐
Plane wave (4)	☐	☐	☐	☐	☐
Multi-mode (5)	☐	☐	☐	☐	☐
Longitudinal wave (6)	☐	☐	☐	☐	☐
Shear wave (7)	☐	☐	☐	☐	☐
Linear scan (8)	☐	☐	☐	☐	☐
Sectorial scan (9)	☐	☐	☐	☐	☐
Other (please specify) (10)	☐	☐	☐	☐	☐
Other (please specify) (11)	☐	☐	☐	☐	☐
Other (please specify) (12)	☐	☐	☐	☐	☐

Q18 Is it assumed that the decision about detection and characterisation of the defect is made manually by the expert performing inspection?

- ○ Yes (1)
- ○ No (2)
- ○ Other (please specify) (3) _____

Q19 What is current resolution of imaging in general, which need to be improved during the project?

_____
_____
_____
_____
_____

End of Block: IMAGING ALGORITHMS

Start of Block: ASSESSMENT PROCEDURE

ASSESSMENT PROCEDURE: Imaging algorithm assessment procedure.

Q20 What improvement is expected in terms of SNR? Quantify it.

- ○ Up to 5% (1)
- ○ Up to 10% (2)
- ○ 10% to 20% (3)
- ○ 20% to 30% (4)
- ○ More than 30% (5)
- ○ This is not a parameter that has to be improved (6)
- ○ Other (please specify) (7) _____

Q21 What improvement is expected in terms of inspection depth? Quantify it.

_____
_____
_____
_____
_____

Q22 What improvement is expected in terms of defect detection? Quantify it.

- ○ Up to 5% (1)
- ○ Up to 10% (2)
- ○ 10% to 20% (3)
- ○ 20% to 30% (4)
- ○ More than 30% (5)
- ○ This is not a parameter that has to be improved (6)
- ○ Other (please specify) (7) _____

Q23 What improvement is expected in terms of defect sizing? Quantify it.

- ○ Up to 5% (1)
- ○ Up to 10% (2)
- ○ 10% to 20% (3)
- ○ 20% to 30% (4)
- ○ More than 30% (5)
- ○ This is not a parameter that has to be improved (6)
- ○ Other (please specify) (7) _____

Q24 What improvement is expected in terms of algorithm performance? Quantify it.

- ○ Up to 5% (1)
- ○ Up to 10% (2)
- ○ 10% to 20% (3)
- ○ 20% to 30% (4)
- ○ More than 30% (5)
- ○ This is not a parameter that has to be improved (6)
- ○ Other (please specify) (7) _____

Q25 What improvement is expected in terms of amount of processing data? Quantify it.

- ○ Up to 5% (1)
- ○ Up to 10% (2)
- ○ 10% to 20% (3)
- ○ 20% to 30% (4)
- ○ More than 30% (5)
- ○ This is not a parameter that has to be improved (6)
- ○ Other (please specify) (7) _____

Q26 What is targeted resolution of the imaging algorithm? Quantify it.

_____

_____
_____
_____

Q27 What is the reference inspection method (gold standard)?

- ○ TRL (4)
- ○ TFM (5)
- ○ Other (please specify) (6) _____

Q28 What is expected trade-off between reduced inspection time and the imaging quality?

- ○ Up to 5% (1)
- ○ Up to 10% (2)
- ○ 10% to 20% (3)
- ○ 20% to 30% (4)
- ○ More than 30% (5)
- ○ Imaging quality should not be reduced while improving the inspection time (6)
- ○ Other (please specify) (7) _____

Q29 Who among the partners should be involved in data acquisition and imaging algorithm assessment?

- ☐ EDF (1)
- ☐ CEA (2)
- ☐ ICL (3)
- ☐ Fraunhoffer (4)
- ☐ UoB (5)
- ☐ M2M (6)
- ☐ KTU (7)
- ☐ Framatome (8)
- ☐ Other (please specify) (9) _____

Q30 Do you think it is relevant to use same data acquisition hardware and processing environment to assess the improvements in proposed imaging algorithms?

- ○ Yes (1)
- ○ No (2)
- ○ Other (please specify) (3) _____

End of Block: ASSESSMENT PROCEDURE

Start of Block: Summary

Q31 What is your role in the Advise project?

- ○ Member of consortium (1)
- ○ Member of IAB (2)
- ○ Other (3) _____

Q32 Please identify your organisation.

- ○ Électricité de France (EDF) (1)
- ○ Imperial College of Science, Technology and Medicine (ICL) (2)
- ○ Fraunhofer Institute for Non-destructive Testing (FRAUNHOFER) (3)
- ○ Commissariat à l'énergie atomique et aux énergies alternatives (CEA) (4)
- ○ University of Bristol (UoB) (5)
- ○ M2M (M2M) (6)
- ○ Bay Zoltán Nonprofit Ltd. for Applied Research (BZN) (7)
- ○ Kaunas University of Technology (KTU) (8)
- ○ Extende (EXT) (9)
- ○ Materials Testing Institute - University of Stuttgart (USTUTT) (10)
- ○ Framatome (11)
- ○ ÚJV Řež, a. s. (UJV) (12)
- ○ Other (please specify) (13) _____

End of Block: Summary

6 Annex 2

THE METHODOLOGY FOR ASSESSMENT OF IMPROVEMENT OF THE IMAGING ALGORITHM

The objective of the methodology is to quantify the improvements of the ultrasonic phased array imaging algorithms proposed throughout the "Advise" project. The methodology presents guidelines for selection of mock-ups, data acquisition set-ups and comparison metrics of imaging techniques. As a result, such methodology brings a unified way to assess the imaging algorithms and to emphasize their benefits.

The methodology is organized in three chapters: mock-ups for inspection; means of data acquisition and measurement set-ups; assessment of the performance of proposed imaging techniques.

1. Mock-ups for assessment of the imaging algorithms

1.1. Description of the mock-ups

The samples for assessment of imaging algorithms were selected from the list of R&D mock-ups[1], provided by the "Advise" project partners. Two potential groups of samples have been distinguished named cast components and welds. The sample selection criteria were based on material/technology, geometry, grain size, type and position of artificial defects. Following mock-ups were selected for further use on imaging algorithm assessment:

1. **Cast components:**
   - Ni based alloy (1618-B359-B1);
   - Static cast stainless steel (D522-TG).
2. **Welds:**
   - V-shape weld (1517-T105EE-2G-GA);
   - Weld repair (1774-T248A).

Each sample is further identified by its unique number. The **1618-B359-B1** is a nickel based alloy (Inconel 600) mock-up, that has 4 side-drilled holes (SDH) (*d* = 2mm) and 2 flat-bottom holes (FBH) (*d* = 4mm and 8mm). The average grain size of the mock-up is 90 µm. **D522-TG** is a coarse grained stainless steel, cast autenoferritic mock-up that possess 5 SDH (*d* = 0.5 mm) and 5 SDH (*d* = 1mm), that are located close to surface of the sample. **1517-T105EE-2G-GA** is a U chamfer, shielded metal manual arc weld with 30 welding passes. It possesses no disorientation in the welding direction and high disorientation of the average grain tilt. 2 SDH (*d* = 1.5 mm) are located the middle of the weld at different depths. **1774-T248A** is a weld cladding repair mock-up, made from Ni based alloy. It has homogeneous microstructure and quasi-vertical grains. Slight grain disorientation at chamfers. The sample has 4 SDH (*d* = 2 mm), 4 vertical notches and 5 tilted notches. The technical drawings of the selected mock-ups are presented in Annex 4.

This methodology was created assuming that the samples listed above will be used for quantification of imaging algorithm performance. Other samples can be used as well, however they should possess parameters close to the ones listed above.

1.2. Description of the targeted defects

The targeted defects in all cases are artificial defects that can be arranged into three groups: side drilled holes (SDH), flat bottom holes (FBH) and notches. The most important characteristics of the defects are ligament, relative position, size (height, diameter) and orientation. The cast mock-ups (**1618-B359-B1** and **D522-TG**) and thin weld (**1517-T105EE-2G-GA**) have SDH as the artificial defects. The SDH in the mock-up **D522-TG** are subsurface defects. They possess small diameter, while the sample itself has a coarse grained structure. The

[1] Advise Mock-up Inventory list. Available online: https://projectsworkspace.eu/sites/Advise/WP1%20deliverables/D1.1%20confidential%20mockup%20inventory/ADVISE_DEL_D1.1.2_IDMWD_R1(2017-12-22).docx

mock-up **1618-B359-B1** has a uniform distribution of grains and additional two FBH's. The thin weld sample **1517-T105EE-2G-GA** has fine grains. The weld repair sample (**1774-T248A**) has SDH's and two types of notches: vertical and tilted. Two notches, one from each group has an opening angle of 3.2°. The detailed description of the positions and sizes of the artificial defects can be seen in Tables 6.2–6.5. The technical drawings of the mock-ups are presented in the Annex 8.

Table 6.2: Detailed positions and sizes of the artificial defects at mock-up 1618-B359-B1

1618-B359-B1	**Dimensions**			**Thickness**	**Width**	**Length**	**Material**
				90 mm	90 mm	285 mm	Inconel 600
	Flaw reference	**SDH10**	**SDH30**	**SDH50**	**SDH70**	**FBH1**	**FBH2**
	Type	Side-drilled hole				Flat-bottom hole	
	Diameter, *d*	2 mm				8 mm	4 mm
	Ligament, *z*	10 mm	30 mm	50 mm	70 mm	70 mm	70 mm
	Height, *h*	–				20 mm	
	Offset from FACE2, *y*	–				60 mm	30 mm
	Offset from FACE1, *x*	30 mm	60 mm	90 mm	120 mm	240 mm	

Table 6.3: Detailed positions and sizes of the artificial defects at mock-up D522-TG

D522-TG	**Dimensions**		**Thickness**	**Width**	**Length**	**Material**
			98 mm	80 mm	598 mm	Stainless steel
	Flaw reference	**SDH5-1**	**SDH10-1**	**SDH15-1**	**SDH20-1**	**SDH30-1**
	Type	Side-drilled hole				
	Diameter, *d*	1 mm				
	Ligament, *z*	5 mm	10 mm	15 mm	20 mm	30 mm
	Offset from FACE3, *x*	70 mm	120 mm	170 mm	220 mm	270 mm
	Flaw reference	**SDH5-0.5**	**SDH10-0.5**	**SDH15-0.5**	**SDH20-0.5**	**SDH30-0.5**
	Type	Side-drilled hole				
	Diameter, *d*	0.5 mm				
	Ligament, *z*	5 mm	10 mm	15 mm	20 mm	30 mm
	Offset from FACE1, *x*	70 mm	120 mm	170 mm	220 mm	270 mm

Table 6.4: Detailed positions and sizes of the artificial defects at mock-up 1517-T105EE-2G

1517-T105EE-2G	**Dimensions**	**Thickness**	**Width**	**Length**	**Material**
		32 mm	70 mm	500 mm	–
	Flaw reference	**SDH10**		**SDH20**	
	Type	Side-drilled hole			
	Diameter, *d*	1.5 mm			
	Ligament, *z*	10 mm		20 mm	
	Offset from FACE1, *x*	250 mm			

Table 6.5: Detailed positions and sizes of the artificial defects at mock-up 1774-T248A

	Dimensions				Thickness	Width	Length	Material
					94 mm	255 mm	396 mm	Ni alloy
1774-T248A	**Flaw reference**	**SDH1**	**SDH2**	**SDH3**	**SDH4**	**EV1**	**EV2**	**EV3**
	Type	Side-drilled hole				Vertical notch		
	Diameter, *d*	1.99 mm	1.99 mm	2.02 mm	2.04 mm	–		
	Ligament, *z*	9 mm	15 mm	15 mm	9.05 mm	0 mm		
	Height, *h*	–				5 mm	10 mm	10 mm
	Width, *w*	–				0.2 mm		
	Tilt angle, *α*	–				90°		
	Length from FACE2, *l*	80 mm				15 mm	15.02 mm	15.01 mm
	Offset from FACE2, *s*	0 mm				95 mm	145 mm	195 mm
	Offset from FACE3, *x*	104 mm	108 mm	159 mm	162 mm	130 mm	130 mm	250 mm
	Flaw reference	**EV4**	**EI1**	**EI2**	**EI3**	**EI4**	**EI5**	
	Type	Vertical notch	Tilted notch					
	Crack opening angle, *γ*	3.2°	–				3.2°	
	Ligament, *z*	0 mm						
	Height, *h*	28.01 mm	5.07 mm	6.53 mm	10.15 mm	5 mm	13.05 mm	
	Width, *w*	–	0.2 mm				–	
	Tilt angle, *α*	90°	80°	50°	80°	50°	80°	
	Length from FACE2, *l*	15.04 mm	15.06 mm	15.02 mm	15.06 mm	15.03 mm	14.99 mm	
	Offset from FACE2, *s*	195 mm	95 mm	95 mm	170 mm	170 mm	220 mm	
	Offset from FACE3, *x*	130 mm	156.5 mm	90 mm	156.5 mm	90 mm	156.5mm	

2. Data acquisition and measurement set-ups

2.1. Measurement set-ups and means of data acquisition

The inspection procedure is selected according to the sample geometry, accessibility, types of defects and their positions. In all cases, inspection is performed using phased arrays. According to the samples defined in previous chapter, several inspection set-ups can be distinguished: direct contact, angle beam, TRL and TOFD. Using the direct contact set-up, the array is positioned directly on the surface of the sample, without wedge. Such set-up is suitable both for SDH and FBH detection that are located sufficiently deep inside the sample. Close to surface SDH's and notches can be detected with angle beam set-ups, using a wedge between the phased array and the mock-up. TRL techniques uses special TRL wedges and pitch-catch technique that allow to improve the signal-to-noise ratio in the coarse grained samples. Such technique is mostly suitable for detection of SDH. The angle of the wedge, frequency of the transducer, number of array elements and position of the array on the mock-up are selected individually for each case by the user, according to their owned equipment, grain structure and defects under inspection. The Tables 6.6–6.9 summarizes

recommended set-ups separately for each of the investigated mock-up and targeted defect. Each set-up has its own data acquisition method, which is either the full matrix capture (FMC) or plane wave excitation (PWE). The user can select one of the recommended set-ups or to define its own set-up if necessary. In any case the order defined in Tables 6.6–6.9 must be maintained. Each set-up leads to a single dataset file, which will be processed by reference and newly developed/modified methods during the project. The datasets will be converted into MFMC format and distributed among project partners for individual processing and analysis.

Table 6.6: Measurement set-ups and data acquisition techniques for mock-up 1618-B359-B1

	Unique set-up no.	Targeted defects	Phased array configuration				Data acquisition method	Dataset file name
			Direct contact (without wedge)	Angle beam (with wedge)	TRL probe	Frequency, *f*		
1618-B359-B1	#01	FBH1–2	+	–	–	2–5 MHz	FMC*	
	#02		+	–	–		PWE**	
	#03	SDH10–70	+	–	–	2–5 MHz	FMC	
	#04		+	–	–		PWE	
	#05		–	+	–		FMC	
	#06		–	–	+		FMC	
	*#ID***							

* – FMC is full matrix capture;

** – PWE refers to plane wave excitation;

*** – Unique set-up defined by the user.

Table 6.7: Measurement set-ups and data acquisition techniques for mock-up D522-TG

	Unique set-up no.	Targeted defects	Phased array configuration			Data acquisition method	Dataset file name
			Angle beam (with wedge)	TRL probe	Frequency, *f*		
D522-TG	#07	SDH5-1–30-1	–	+	1–3 MHz	FMC	
	#08		+	–	1–3 MHz	FMC	
	#09		+	–		PWE	
	#10	SDH5-0.5–30-0.5	–	+	1–3 MHz	FMC	
	#11		+	–	1–3 MHz	FMC	
	#12		+	–		PWE	
	#ID						

Table 6.8: Measurement set-ups and data acquisition techniques for mock-up 1517-T105EE-2G

	Unique set-up no.	Targeted defects	Phased array configuration			Data acquisition method	Dataset file name
			Angle beam (with wedge)	TRL probe	Frequency, *f*		
1517-T105EE-2G	#13	SDH10–20	–	+	2–5 MHz	FMC	
	#14	SDH10–20	+	–	2–5 MHz	FMC	
	#15		+	–		PWE	
	#ID						

Table 6.9: Measurement set-ups and data acquisition techniques for mock-up 1774-T248A

	Unique set-up no.	Targeted defects	Phased array configuration				Data acquisition method	Dataset file name
			Angle beam (with wedge)	TRL probe	TOFD	Frequency, *f*		
1774-T248A	#16	SDH1–4	–	+	–	2–5 MHz	FMC	
	#17		+	–	–			
	#18	EV1–4	–	+	–	2–5 MHz	FMC	
	#19		+	–	–			
	#20		–	–	+			
	#21	EI1–5	–	+	–	2–5 MHz	FMC	
	#22		+	–	–			
	#23		–	–	+			
	#ID							

2.2 Processing of the acquired data sets

After acquisition of the data, two imaging techniques must be applied to the same dataset: A reference and the one to be quantified. The reference imaging method depends on the data acquisition method. I.e. for FMC acquisition, total focusing method (TFM) is used as a reference imaging method. For PWE set-ups, plane wave imaging (PWI) techniques are used as reference. Then the user should apply the newly proposed imaging technique to the same dataset in order to be able to quantify the improvement. The Table 6.10 presents the reference processing methods for each data acquisition set-up, which was identified previously.

Table 6.10: Processing of acquired data sets using reference and improved algorithms

Unique sample identifier	Unique set-up no.	Dataset file name	Reference imaging method	Imaging method to be quantified	Processed data file (image)
1618-B359-B1	#01		TFM		
	#02		PWI		
	#03		TFM		
	#04		PWI		
	#05		TFM		
	#06		TFM		
	#ID				
D522-TG	#07		TFM		
	#08		TFM		
	#09		PWI		
	#10		TFM		
	#11		TFM		
	#12		PWI		
	#ID				
1517-T105EE-2G	#13		TFM		
	#14		TFM		
	#15		PWI		
	#ID				

Table 6.10: Processing of acquired data sets using reference and improved algorithms (continued)

1774-T248A	#16		TFM		
	#17				
	#18				
	#19				
	#20				
	#21				
	#22				
	#23				
	#ID				

3. Assessment of the performance of proposed imaging techniques

3.1. Comparison of the processing methods and parameters

Since the reference and the quantified methods are applied on the same dataset, which was acquired using the same set-up and hardware, it's possible to measure the improvement of the newly proposed imaging techniques. Following parameters can be distinguished for the assessment of imaging algorithm performance: detectability of the defect, inspection depth, signal to noise ratio (SNR) or contrast to noise ratio (CNR), ligament, height and tilt angle. The quantification parameters depend on the type of the defect that has been investigated. The most important parameter is the detectability of the defect, which identifies if the defect can be detected in general. It's a binary parameter, identifying whether the particular defect is visible in the reconstruction. The inspection depth defines the maximum depth at which the defect can be clearly observed. In the ideal case, the inspection depth is equal to the thickness of the sample. The quality of ultrasonic imaging is defined by the fact how clearly the reflections of defects under investigation appear above the background noise. This can be expressed in terms of SNR or CNR. However, many different approaches to obtain SNR/CNR values exist, which sometimes lead to inconsistent and contradicting results. A special study has been prepared on SNR/CNR evaluation approaches and their performance in different scenarios, which is presented in Annex 3. Ligament defines the depth of the defect with respect to the inspection surface and is applied to SDH and FBH. The notch type defects have two additional parameters namely height and tilt angle (for tilted notches). Parameters for comparison of the imaging methods are presented in Table 6.11.

Table 6.11: Parameters for comparison of the imaging methods

Unique sample identifier	**Unique set-up no.**	**Processed data file (image)**	**Reference imaging method performance**				**Quantified imaging method performance**			
			Detectability	**Inspection depth**	**SNR/CNR**	**Ligament**	**Detectability**	**Inspection depth**	**SNR/CNR**	**Ligament**
1618-B359-B1	#01									
	#02									
	#03									
	#04									
	#05									
	#06									
	#ID									

Table 6.11: Parameters for comparison of the imaging methods (continued)

			Reference imaging method performance				Quantified imaging method performance			
D522-TG	**Unique set-up no.**	**Processed data file (image)**	**Detectability**	**Inspection depth**	**SNR/CNR**	**Ligament**	**Detectability**	**Inspection depth**	**SNR/CNR**	**Ligament**
	#07									
	#08									
	#09									
	#10									
	#11									
	#12									
	#ID									
			Reference imaging method performance				**Imaging method performance**			
1517-T105EE-2G	**Unique set-up no.**	**Processed data file (image)**	**Detectability**	**Inspection depth**	**SNR/CNR**	**Ligament**	**Detectability**	**Inspection depth**	**SNR/CNR**	**Ligament**
	#13									
	#14									
	#15									
	#ID									

			Reference imaging method performance						Imaging method performance					
1774-T248A	**Unique set-up no.**	**Processed data file (image)**	**Detectability**	**Inspection depth**	**SNR/CNR**	**Ligament**	**Height**	**Tilt angle**	**Detectability**	**Inspection depth**	**SNR/CNR**	**Ligament**	**Height**	**Tilt angle**
	#16						–	–					–	–
	#17						–	–					–	–
	#18					–		–				–		–
	#19					–		–				–		–
	#20					–		–				–		–
	#21					–						–		
	#22					–						–		
	#23					–						–		
	#ID													

3.2 Assessment of the improvement of the proposed imaging algorithm

The achieved improvement of the proposed imaging algorithm in comparison with reference method can be summarized with Table 6.12. It's common that the improvement will be achieved with some of the parameters only. In any case, the following table enables to clearly identify the fields of improvement of the newly proposed imaging methods.

Table 6.12: Summary of the achieved imaging improvement

	Unique sample identifier	Unique set-up no.	Estimated value with reference method	Estimated value with quantified method	Achieved improvement
Detectability					
Inspection depth					
SNR					
Ligament					
Height					
Tilt angle					

7 Annex 3

STUDY OF NOISE ASSESSMENT TECHNIQUES

The Advise project aims to develop advanced signal and data processing algorithms that enable to improve the detection and assessment of the defects in the complex materials. The problem is that such materials possess a granular structure which in the case of ultrasonic inspections generates structural noise concealing the response of the defects. Throughout the project several methods of ultrasonic inspection and imaging are being developed. Hence one of the tasks is to assess and compare proposed methods with respect to the achieved improvement. At a first glance, this task looks rather simple; however there is big variety of methods for the assessment of ultrasonic images and the quality of the inspection. The study presented in this chapter aims to compare different SNR and CNR evaluation approaches and to discuss their performance and limitations.

1. The methods for assessment of ultrasonic images

The ultrasonic images obtained during inspection of a particular object usually contain some features which can be defined as follows:

1. **The background**, which can be classified as noise. It is mainly related to the structural properties of materials such as grain size and orientation, porosity, inter-granular micro-cavities, anisotropy etc. It is also affected by the parameters of the ultrasonic system such as central frequency, bandwidth, gain level. However, in this study we do not analyse the origin of this background noise.
2. **The indication**, which is related to the geometrical feature of the object that provides sufficiently strong reflection compared to the background noise, however these are not actual defects. The example of such signals or indications in the ultrasonic images can be backwall reflection, corner reflections or reflections from other geometrical features.
3. **The indications** which are expected to be the reflections from defects. These particular indications are the object of the inspection, which need, to be detected. In the case of the reference samples, the reflections from defects are artificial ones, i.e. side drill hole (SDH) or flat bottom holes (FBH).

In general, the quality of ultrasonic imaging is defined by the fact how clearly the reflections of defects appear above the background noise. So, the aim of this study is to determine what parameters shall be used to describe the appearance of indications in most reliable way.

The following parameters have been analysed for assessment of the ultrasonic image quality:

1. The **conventional signal to noise ratio** (SNR) SNR_1

$$\mathrm{SNR}_1 = 20\log_{10}\left(\frac{\max(S(x,y))}{\max(N(x,y))}\right), \tag{7.1}$$

where $S(x,y)$is the signal in a particular area in the ultrasonic image corresponding to the indication under analysis; $N(x,y)$ is the noise in a particular area. It is assumed that the noise region is free from any indications. So, this parameter defines the SNR as ratio of the maximal amplitude of the indication and maximal amplitude of the noise. It is necessary to state that such assessment parameter does not take into account parameters other than the indication and noise. As the area of the noise can be quite large compared to the area of indication the appearance of higher amplitudes of the noise in any point of this area can lead to a non-correct assessment. Probably it should be recommended to select the area of the noise only around or in close proximity of the indication.

2. The **signal to mean noise ratio** SNR_2 calculated according to

$$\mathrm{SNR}_2 = 20\log_{10}\left(\frac{\max(S(x,y))}{\mathrm{mean}(N(x,y))}\right), \tag{7.2}$$

The difference to the previous definition is that for assessment of the noise mean values are used rather than maximum values.

3. The **signal to mean squared noise ratio** SNR_3 calculated according to

$$\mathrm{SNR}_3 = 20\log_{10}\left(\frac{\max(S(x,y))}{\sqrt{\mathrm{mean}(N(x,y)^2)}}\right). \tag{7.3}$$

4. The **contrast to noise ratio** CNR_1 calculated according

$$\mathrm{CNR}_1 = \frac{\left(\mathrm{mean}(S(x,y)) - \mathrm{mean}(N(x,y))\right)}{\mathrm{std}(N(x,y))}. \tag{7.4}$$

Instead of maximum values, this parameter uses the difference ratio (contrast) between mean values of signal and noise with respect to noise standard deviation.

5. The signal to noise ratio SNR_4 calculated according

$$\mathrm{SNR}_4 = 20\log_{10}\left(\frac{\max(S(x,y))}{\max(I(x,y))}\right), \tag{7.5}$$

This parameter is related to the analysis of the particular image instead of the noise. It defines how bright the indication appears in the image. The idea behind this parameter is that the colour scale can be changed during the analysis. By changing this scale, the brightness of the indication varies essentially. Incorrect set-up of the colour scale can lead to loss of the indication, or to the appearance of artefacts with relatively low amplitude. The SNR_4 determines the ratio between the indication and reference reflector, however the colour scale should be set to some particular value determined during calibration on reference sample. So, this particular parameter can be used not only for image assessment, but also acceptance criteria for inspection.

2. Samples selected for analysis

Three types of samples were selected for analysis of the noise. The first one is coarse grained stainless steel mock-up **RDIM3** with high structural noise. The other two mock-ups **1618-B359-B1** and **1618-B359-B3** possess relatively fine grained structures and correspondingly low structural noise. Such different samples have been selected with the purpose of demonstrating two essentially different cases (coarse grain and quite transparent samples) demonstrating the possibility to assess image quality and at the same time to compare different image processing or reconstruction techniques. The mock-up **RDIM3** is a segment of a pipe with radius of 400 mm. It has a coarse grained homogenous structure of 18% fine grain (grain diameter = 0.3mm) in a matrix of 82% coarse grain (grain diameter = 2.4mm). The average grain size of the sample is expected to be approx. 2mm. Five flat bottom holes of 3mm diameter are located at different depths as target defects in this mock-up as it can be seen in Figure 7.1a. The exact defect positions and their offsets with respect to the reference (left) edge are summarized in Table 7.1. For the SNR-CNR evaluation, the flat bottom hole referenced as “D” will be further analysed as it is located at sufficient depth to generate high backscattering noise and low reflection from the defect itself. The mock-ups **1618-B359-B1** and **1618-B359-B3** are nickel based alloys (Inconel 600), which have average grain sizes of 90 µm and 750 µm respectively. Each of them has 4 side-drilled holes (SDH) (d = 2mm) located at depths 10mm, 30mm, 50mm, 70mm and 2 flat-bottom holes (FBH) (d = 4mm and 8mm) situated at the bottom of the mock-up. The drawing of the mock-ups ups **1618-B359-B1** and **1618-B359-B3** with defect locations can be seen in Figure 7.1b.

Table 7.1: Defect positions at sample RDIM3

Defect reference	A	B	C	D	E
Ligament (mm)	10	20	40	60	80
Offset from left egde (mm)	60	120	180	240	338

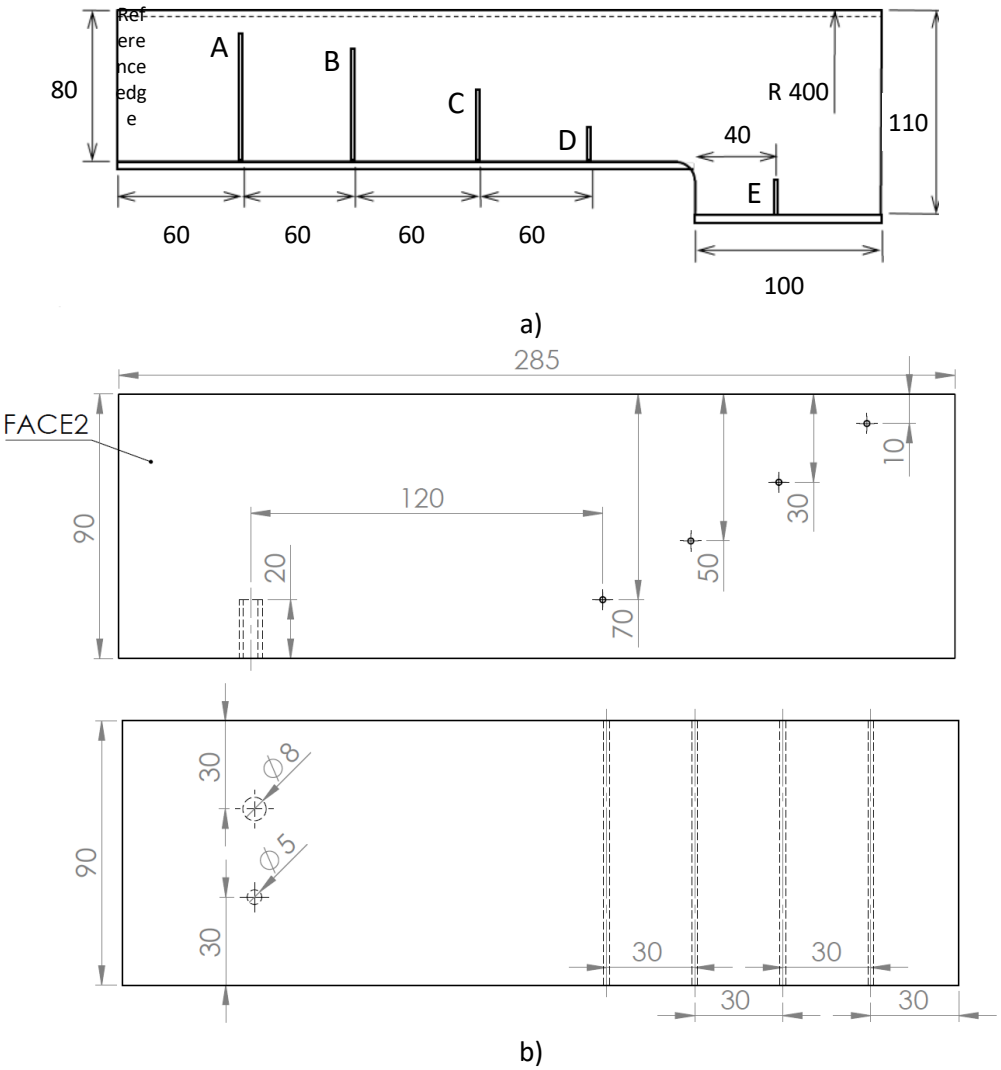

Figure 7.1 The schematic diagram of the mock-up RDIM3 (a) and 1618-B359-B1 (b): geometry and locations of the FBH defects

3. Data Acquisition

For acquisition of the measurement data, a pair of 1MHz 32 elements phased arrays were used in a TRL set-up. Custom 0° incidence TRL wedges with cylindrical surface were manufactured as can be seen in Figure 7.2. The wedges possess roof angles of 10° and provide a beam convergence point at 62.6mm depth. The acquisition of the data was performed using three different modes:

1. **Conventional full matrix capture** (FMC). In this case, one element of transmitting array was used for excitation while all elements of receiving array were used for acquisition. Such procedure was repeated for each element of the transmitter.
2. **Reversed acquisition**, where full matrix capture is performed twice, switching transmitting and receiving arrays. In this procedure, two FMC datasets are acquired. It means that previous

transmitter becomes a receiver in the second FMC dataset. Due to reciprocity principle, instead of averaging two FMC datasets, they are combined in a slightly different way. Suppose that for i^{th} transmitter and j^{th} receiver we have two time signals t_1 and t_2. To get "averaged" signal for this transmitter-receiver pair we compare each sample between signals t_1 and t_2 and output the minimum sample value. So the "averaged" signal t contains minimum values from t_1 and t_2.

3. **Full matrix capture using two elements of array for excitation and all elements for reception**. In this case we excite two elements of transmitting array and use all elements of receiving array. Then the elements of transmitter are shifted by one element and the acquisition is repeated. The main difference from classic TFM is that two elements are fired at each step instead of one.

Using the reversed acquisition described at point 2 above, the two FMC datasets are combined selecting minimal sample values between two signals for each transmitter-receiver pair:

$$y_{n_i,k_j}(t_m) = \begin{cases} y_{1,n_i,k_j}(t_m) & if \ \left|y_{1,n_i,k_j}(t_m)\right| < \left|y_{2,n_i,k_j}(t_m)\right| \\ y_{2,n_i,k_j}(t_m) & otherwise \end{cases} \quad (7.6)$$

where $y_{n_i,k_j}(t_m)$ – is the output magnitude value of i^{th} and j^{th} signal at time instance t_m, $y_{1n_i,k_j}(t_m)$ and $y_{2n_i,k_j}(t_m)$ – are the magnitude values of at point (i,j) at time instance t_m that correspond to the first and second FMC acquisition respectively, i=1,...I, where I is the total number of measurement positions on the n axis, j=1,...J, where J is the total number of measurement positions on k axis, m=0,...M, where M is the number of samples of the signal. The procedure of reversed excitation is described in Figure 7.3.

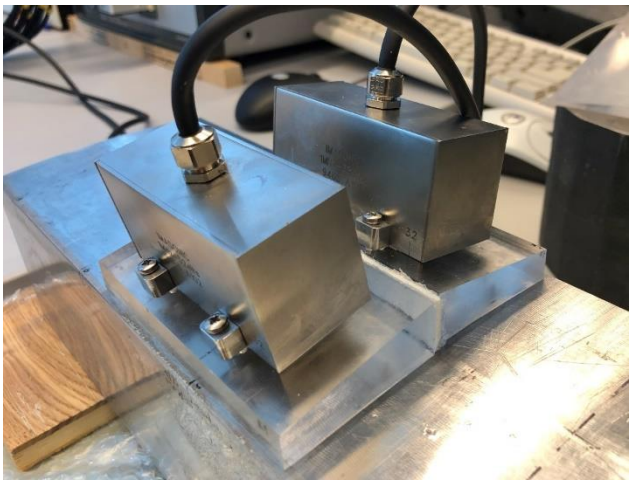

Figure 7.2 0° incidence TRL wedge for inspection of convex samples with FBH

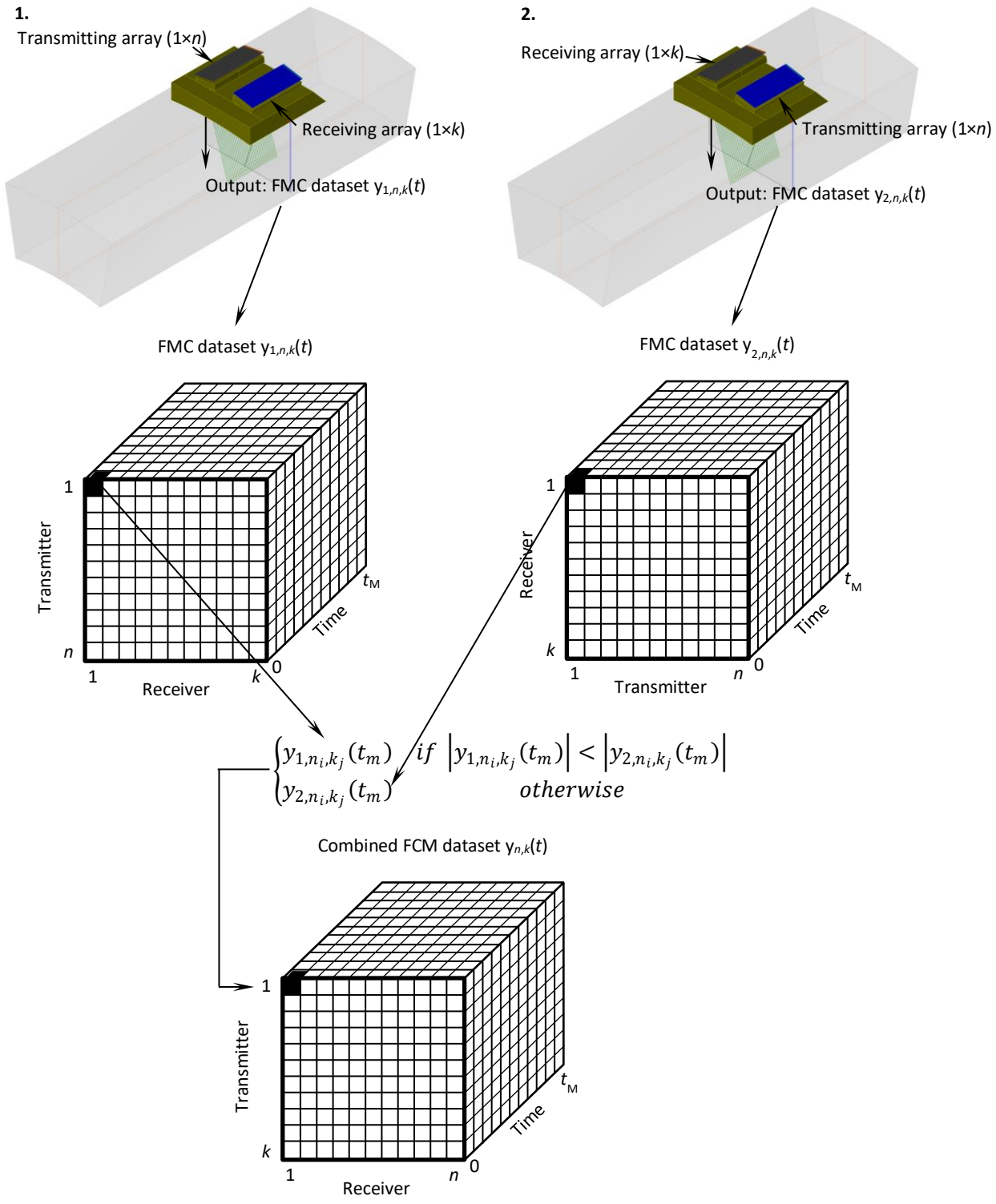

Figure 7.3 Explanation of the reversed excitation and estimation of the combined FMC dataset from two separate FMC acquisitions

4. Analysed reconstructions

All acquired datasets were reconstructed using the total focusing method. Each image is normalized with respect of maximal value (back wall reflection) and the colour scale was limited to 0.1. All the analysed datasets can be seen from Figure 7.4 to Figure 7.6.

Figure 7.4 represents two analysed reconstructions, acquired using classic full matrix capture technique. The first part in Figure 7.4 is a classic TFM reconstruction without any further processing, while the second part

uses an additional filtering by supressing higher frequencies in order to reduce excitation induced noise of the transmitting elements.

Figure 7.5 shows another two reconstructions from reversed excitation measurement. Again, the first part is a classic TFM reconstruction,while the second part uses the same filter as described previously. Finally, Figure 7.6 shows a classic TFM reconstruction of an FMC acquisition where two array elements were used for excitation and all elements for the reception. All presented images visually look very similar. Indications of flat bottom reflection in the images presented in Figure 7.4 looks relatively bright, however the background noise is also strong and non-uniform. The images obtained using reverse excitation possess more uniform noise, which is significantly reduced when some filtering was applied. However, the indications of the flat bottom hole are less bright compared to Figure 7.4. In the case of FMC using excitation of pairs of elements the noise is reduced and indications appear relatively clear. This evaluation is only visual and as a consequence is subjective, so it is very important to look at the actual metrics obtained by the noise evaluation parameters mentioned above.

The images obtained on the fine grain samples B1 and B3 are presented Figure 7.7 and Figure 7.8 respectively. In both cases conventional TFM was used for image reconstruction. The very low background noise can be observed in both images and there are only minor differences between them neglecting that sample B3 possess essentially bigger grain. Of course it is necessary to take into account that sample B3 was measured using 10dB higher gain. The images are slightly shifted along the x axis due to a different position of phased array on the sample.

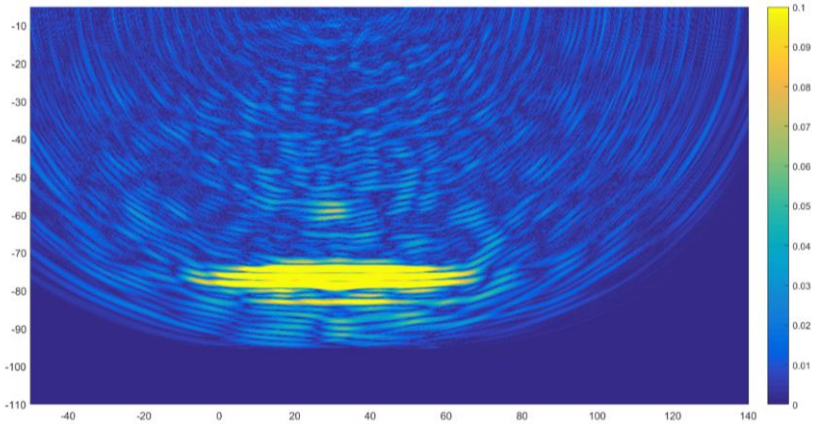

a)

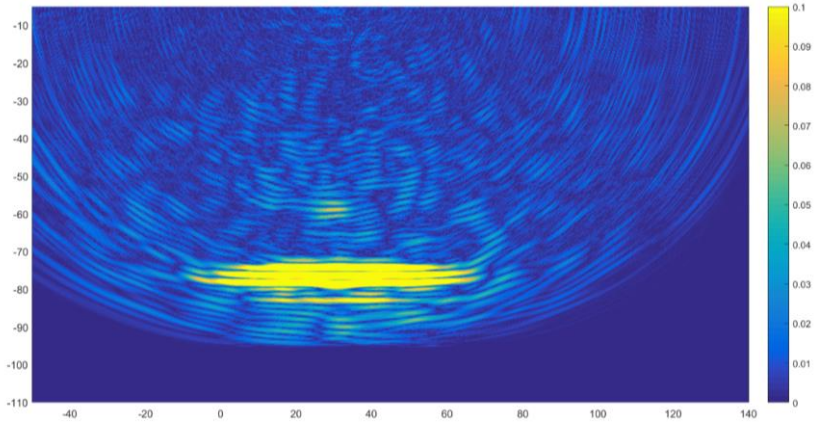

b)

Figure 7.4 TFM reconstruction of conventional FMC datasets: conventional TFM (a) and TFM with additional filtering to reduce reverberations of the transmitting element (b)

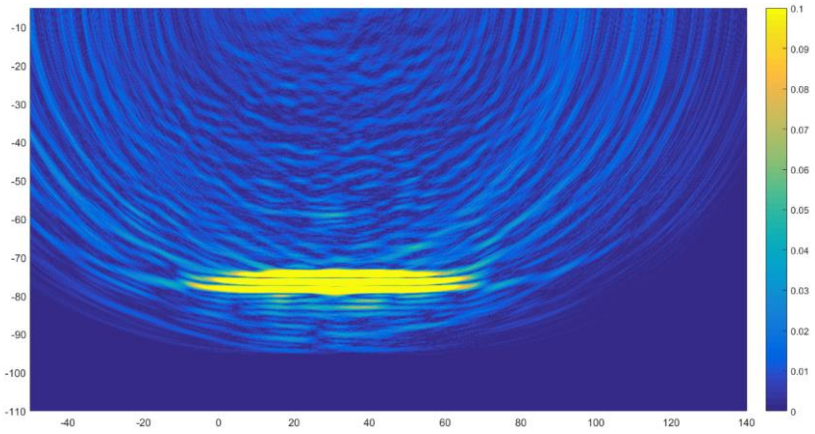

a)

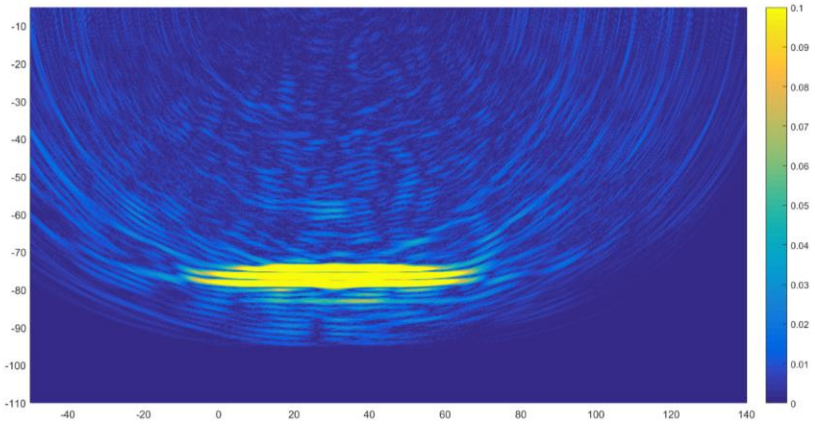

b)

Figure 7.5 TFM reconstruction of FMC datasets acquired using reversed excitation: conventional TFM (a) and TFM with additional filtering to reduce reverberations of the transmitting element (b)

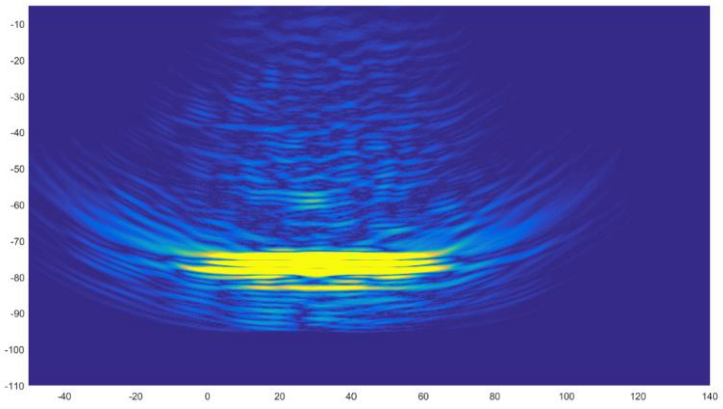

Figure 7.6 Conventional TFM reconstruction of FMC datasets where two elements were used for excitation

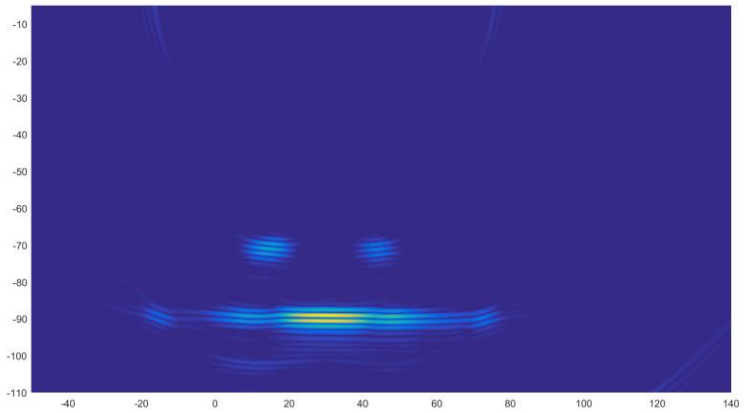

Figure 7.7 The image obtained on the sample B1 using conventional FMC. The right one correspond to 2mm diameter FBH, the left one- 3mm.

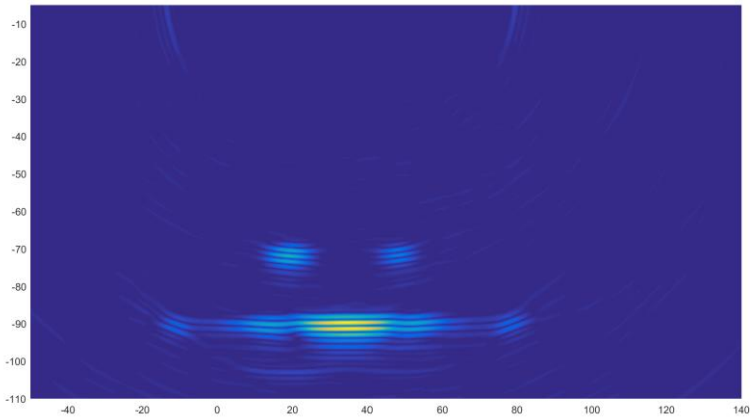

Figure 7.8 The image obtained on the sample B3 using conventional FMC The right one correspond to 2mm diameter FBH, the left one- 3mm.

5. Window positions

All of the noise evaluation methods presented above require selection of some particular zone in the image. The most important choice, which on other hand is not strictly defined, is the zone for the estimation of the noise parameters. The zone for indication is more obviously determined and only minor deviations of window position and size can be expected. So, several different window positions were selected for SNR-CNR analysis on images of RDIM3 sample. These windows used for analysis of coarse grain sample are illustrated in Figure 7.9 and for fine grain sample in Figure 7.10. Each analysed window position is referenced as “case 1”, “case 2” and “case 3”.

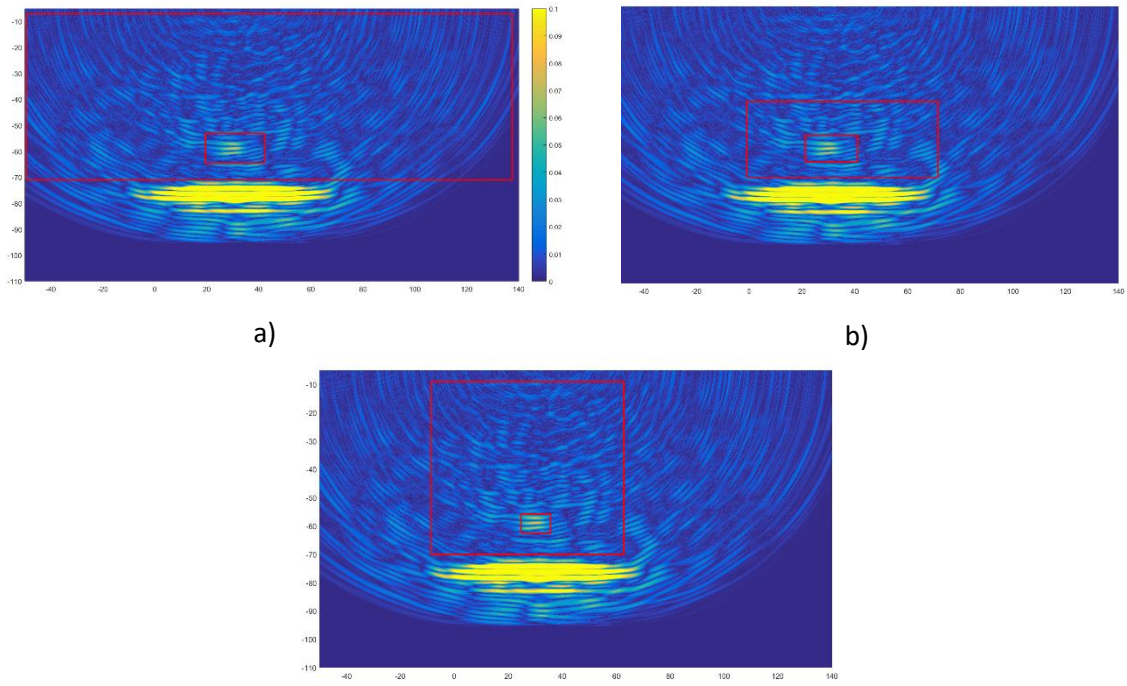

a) b)

c)

Figure 7.9 Analysed window positions for calculation of SNR and CNR values on the images obtained on coarse grain sample: case 1 (a), case 2(b), case 3 (c)

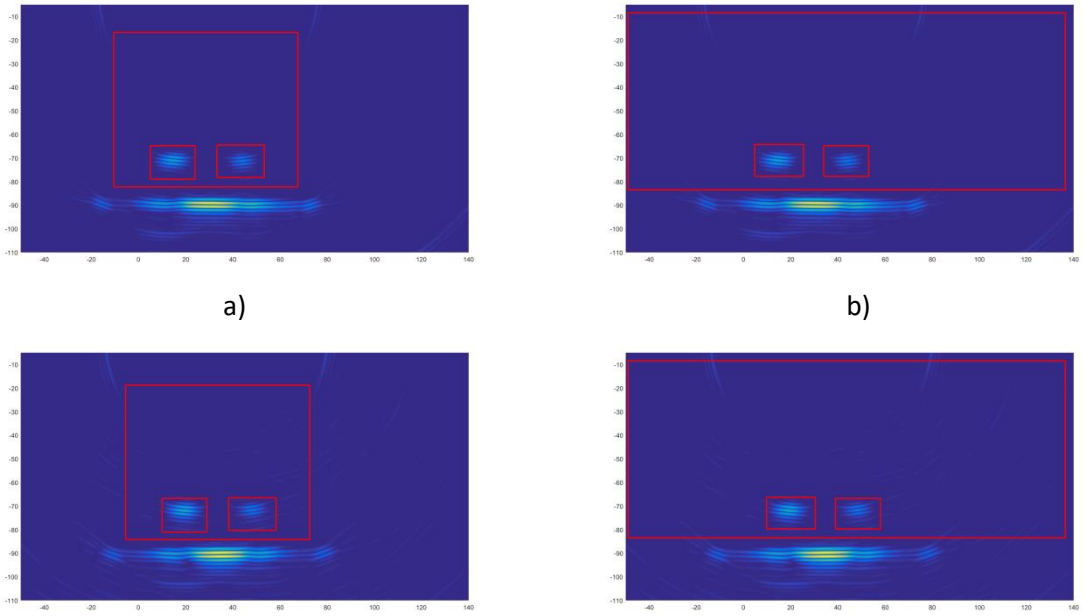

a) b)

c) d)

Figure 7.10 Analysed window positions for calculation of SNR and CNR values on the images obtained on fine grain samples B1 and B3: case 1 (a and c), case 2(b and d)

The positions of the windows were selected manually, without particular intentions- just to take different windows. The coordinates of the selected windows are presented in Table 7.2 for the coarse grain sample and in Table 7.3 and Table 7.4 for the fine grain sample. In the tables P_{11} and P_{12} denote lower left and upper write corners of the window for noise evaluation, while P_{21}, P_{22}, P_{31}, P_{32} denote the corresponding corners of the window for indications. For the images of samples B1 and B3 only two cases of the windows were analysed however the windows are slightly different for both samples due to different positions of the phased array on the sample during data acquisition.

Table 7.2: The corner coordinates of the windows for signal and noise analysis in the case of images obtained on the coarse grain sample RDIM3

Case		P_{11},mm	P_{12},mm	P_{21},mm	P_{22},mm
Case 1	*x*	-49	138	20	40
	z	-71	-7	-65	-53
Case 2	*x*	-1	72	21	41
	z	-70	-41	-64	-54
Case 3	*x*	-8	63	25	36
	z	-70	-9	-62	-56

Table 7.3: The corner coordinates of the windows for signal and noise analysis in the case of images obtained on the fine grain sample 1618-B359-B1

	P_{11},mm	P_{12},mm	P_{21},mm	P_{22},mm	P_{31},mm	P_{32},mm
x	-49	137	5	26	34	53
z	-93	-9	-78	-64	-78	-64

Table 7.4: The corner coordinates of the windows for signal and noise analysis in the case of images obtained on the fine grain sample 1618-B359-B3

	P_{11},mm	P_{12},mm	P_{21},mm	P_{22},mm	P_{31},mm	P_{32},mm
x	-49	137	10	31	39	58
z	-93	-9	-80	-66	-80	-67

6. Evaluation of SNR and CNR

The estimated signal to noise ratios obtained according to the equations given in chapter 2 as well as statistical characteristic of the noise – mean value and standard deviation for all three cases - are presented in Table 7.5 and Table 7.6. The SNR_4 is shown in the table only for the case 1 as it does not depend on dimensions of the window selected for noise.

Table 7.5: The SNR and CNR evaluation results on coarse grain sample RDIM3

FMC acquisition	TFM processing	Window position	SNR_1, dB	SNR_2, dB	SNR_3, dB	CNR_1, dB	SNR_4, dB	Mean noise	Standard deviation of noise
Conventional FMC	Conventional TFM	Case 1	4	21	19	2	-1	0.0079	0.0065
		Case 2	4	18	16	1		0.0117	0.0090
		Case 3	4	19	17	3		0.0098	0.0078
	TFM with filtering	Case 1	5	22	19	2	-1	0.0076	0.0064
		Case 2	5	18	16	1		0.0114	0.0088
		Case 3	5	20	18	3		0.0092	0.0075
Reversed FMC	Conventional TFM	Case 1	0	16	15	0	-5	0.0082	0.0062
		Case 2	0	15	13	0		0.0101	0.0074
		Case 3	0	16	15	1		0.0083	0.0059
	TFM with filtering	Case 1	0	19	17	1	-7	0.0051	0.0045
		Case 2	0	17	14	1		0.0069	0.0055
		Case 3	0	19	17	2		0.0052	0.0045
FCM with two element excitation	Conventional TFM	Case 1	3	26	21	2	-3	0.0033	0.0049
		Case 2	3	19	16	1		0.0080	0.0068
		Case 3	3	22	19	4		0.0058	0.0057

Table 7.6: The SNR and CNR evaluation results on fine grain sample B1 and B3

	SNR_1,dB	SNR_2,dB	SNR_3,dB	CNR_1,dB	SNR_4,dB	Mean noise	Standard deviation of noise
Sample B1, FBH 3mm (case 1)	24	39	38	22	-8	0.0033	0.0049
Sample B1, FBH 2mm (case 1)	19	34	33	10	-13	0.0033	0.0049
Sample B1, FBH 3mm (case 2)	19	39	38	17		0.0080	0.0004
Sample B1, FBH 2mm (case 2)	14	34	33	9		0.0080	0.0004
Sample B3, FBH 3mm (case 1)	25	35	34	14	-7	0.0047	0.0019
Sample B3, FBH 2mm (case 1)	19	29	28	6	-13	0.0047	0.0019
Sample B3, FBH 3mm (case 2)	18	35	34	12		0.0048	0.0024
Sample B3, FBH 2mm (case 2)	11	29	28	6		0.0048	0.0024

7. Discussion

The obtained results can be summarised as follows:

1. The SNR_1 shows that the best signal to noise ratio in the case of the coarse grain sample is associated to the image obtained by TFM with additional filtering (Figure 7.4 b). Other processing algorithms demonstrate lower SNR_1, especially low (SNR_1=0) for reverse excitation case.
2. In the case of samples B1 and B3 the SNR_1 shows very similar results: for 3mm FBH SNR_1=24-25dB, for 2mm FBH SNR_1=19dB. In the case where a wide window is used for the estimation of the noise, SNR_1 for both FBH is reduced roughly by 5-6dB. This can be explained by the fact that the wider window covers some wave indication on the edges of phased array, which leads to overestimation of the noise.
3. The SNR_2 shows a similar trend on coarse grain sample, however the best results (for all window sizes) are demonstrated by the image obtained using two elements excitation (Figure 7.6). The SNR_2 obtained using different windows is quite different (varies in the range up to 7dB), but does however show the same trend. In general, the values of SNR_2 are about 10-15 higher compared to SNR_1.
4. On samples B1 and B2 the SNR_2 show exactly the same trend as SNR_1, the values are just 10-15dB higher.
5. The SNR_3 shows the same trend on all samples as SNR_2, with just slightly smaller values.
6. For the coarse grain samples, the CNR_1 gives almost identical results for images in Figure 7.4 and Figure 7.6. Only in the window case 3 the evaluation of the image in Figure 7.6 is 1dB higher. The variation of the CNR_1 for different cases and different techniques varies very little, but not more than 4dB. In the window case 2 there completely no difference (CNR_1=1). In the case of fine grained samples B1 and B3, CNR_1 shows very good results, whereas amplitude of the signal reflected by 3 mm FBH is roughly 10 dB higher compared to reflection from 2 mm FBH.
7. The SNR_4 shows as best both images in Figure 7.4. So, in general fits with SNR_1.

8. Conclusions of the chapter

1. For images with strong structural noise, SNR_1 and SNR_4 give better assessment of the signal to noise ratio
2. SNR_2 and SNR_3 give close, but not completely identical results compared to SNR_1. The differences can be expected when there are minor differences between noise of the images.
3. CNR_1 shows very good dependency on the diameter of FBH in the case of low noise images. However, in the case of noisy images the sensitivity of CNR_1 is very low and can lead to ambiguities in the assessment.
4. The user has to be aware of differences between different SNR estimations and deliberately select ones that fits to a specific needs. The consistency is important while comparing the performance of different imaging techniques.

8 Annex 4

Sample 1618-B359-B1

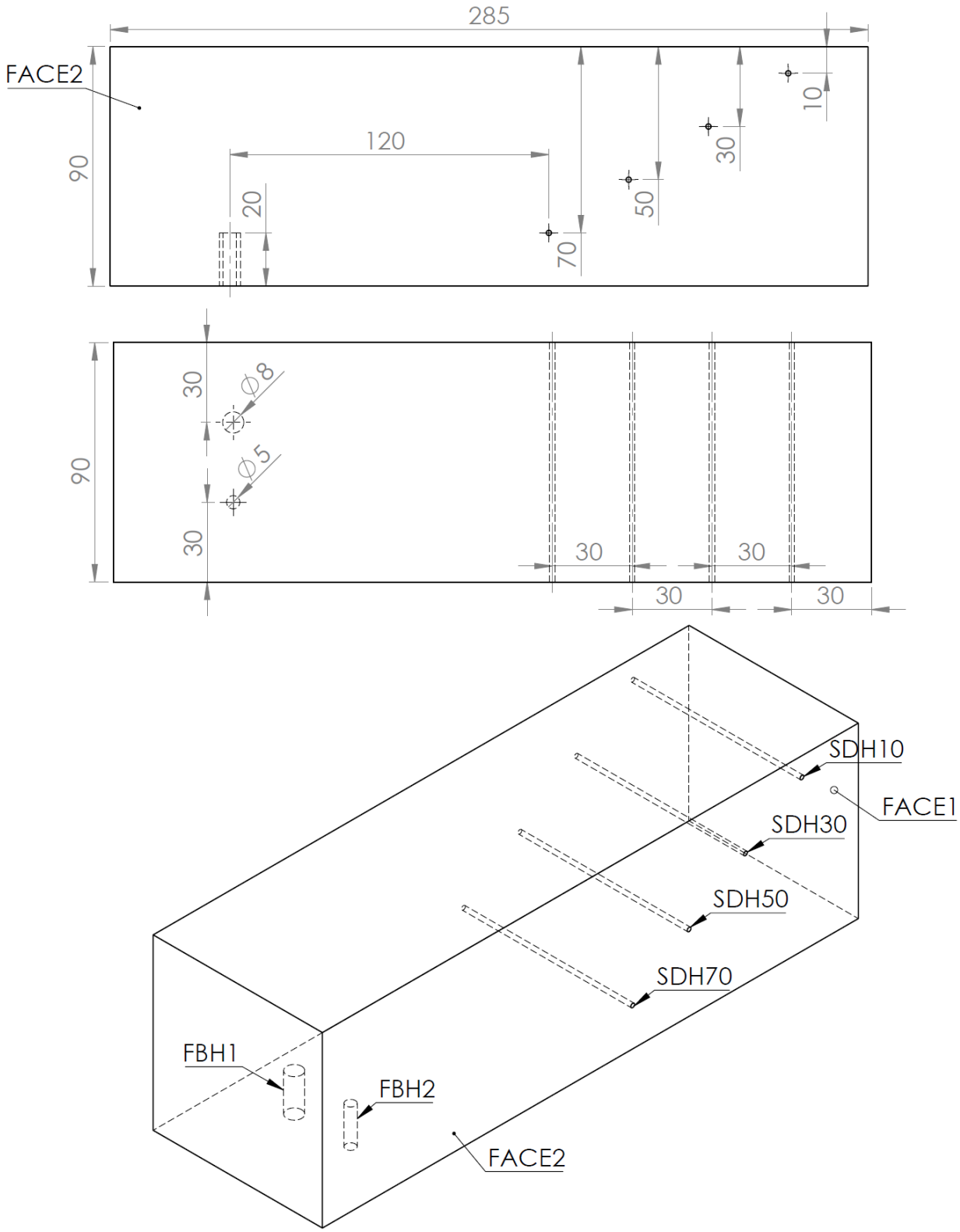

Figure 8.1: The sketch of the mock-up 1618-B359-B1

Sample D522-TG

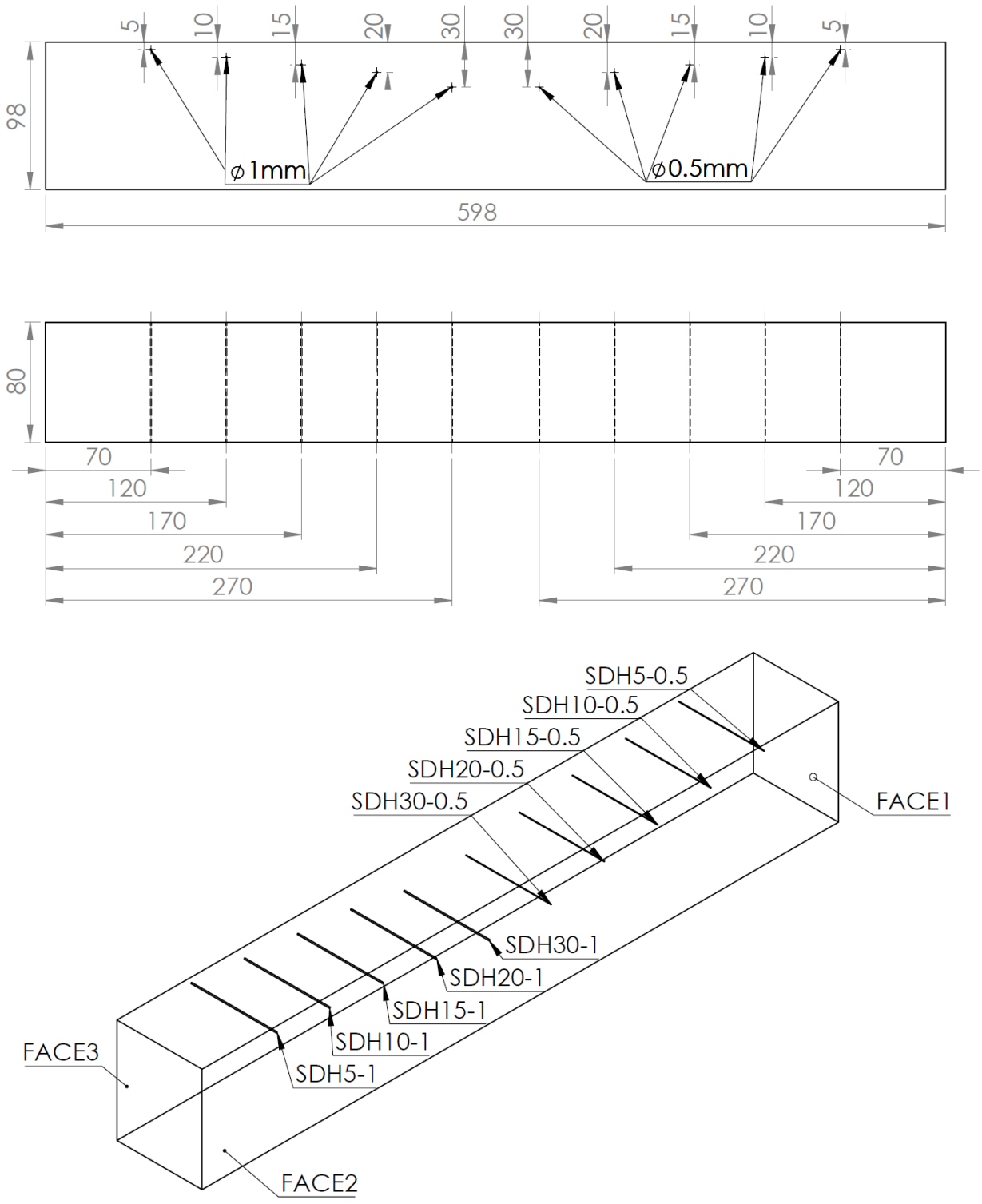

Figure 8.2: The sketch of the mock-up D522-TG

Sample 1517-T105EE-2G-GA

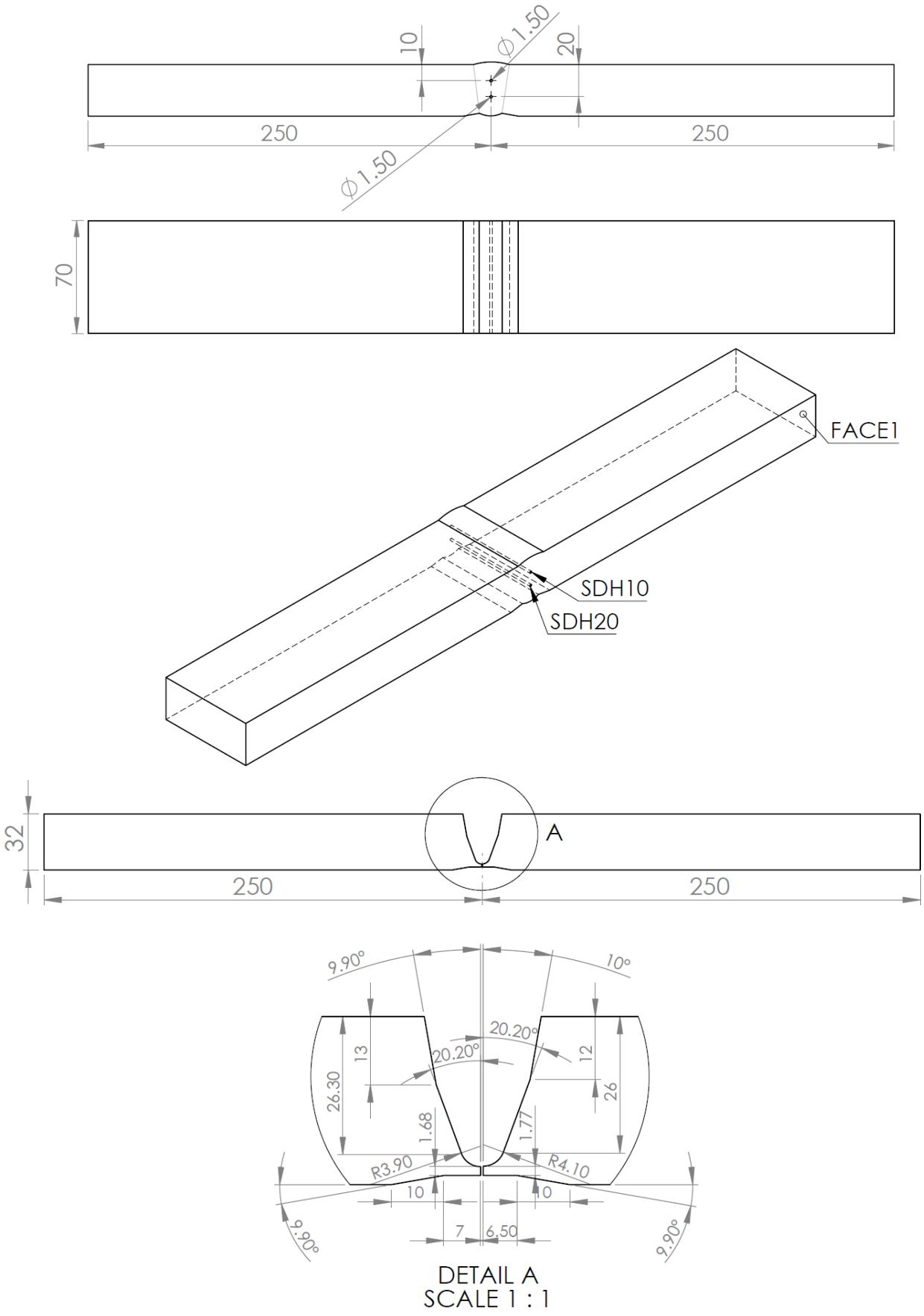

Figure 8.3: The sketch of the mock-up 1517-T105EE-2G-GA

Sample 1774-T248A

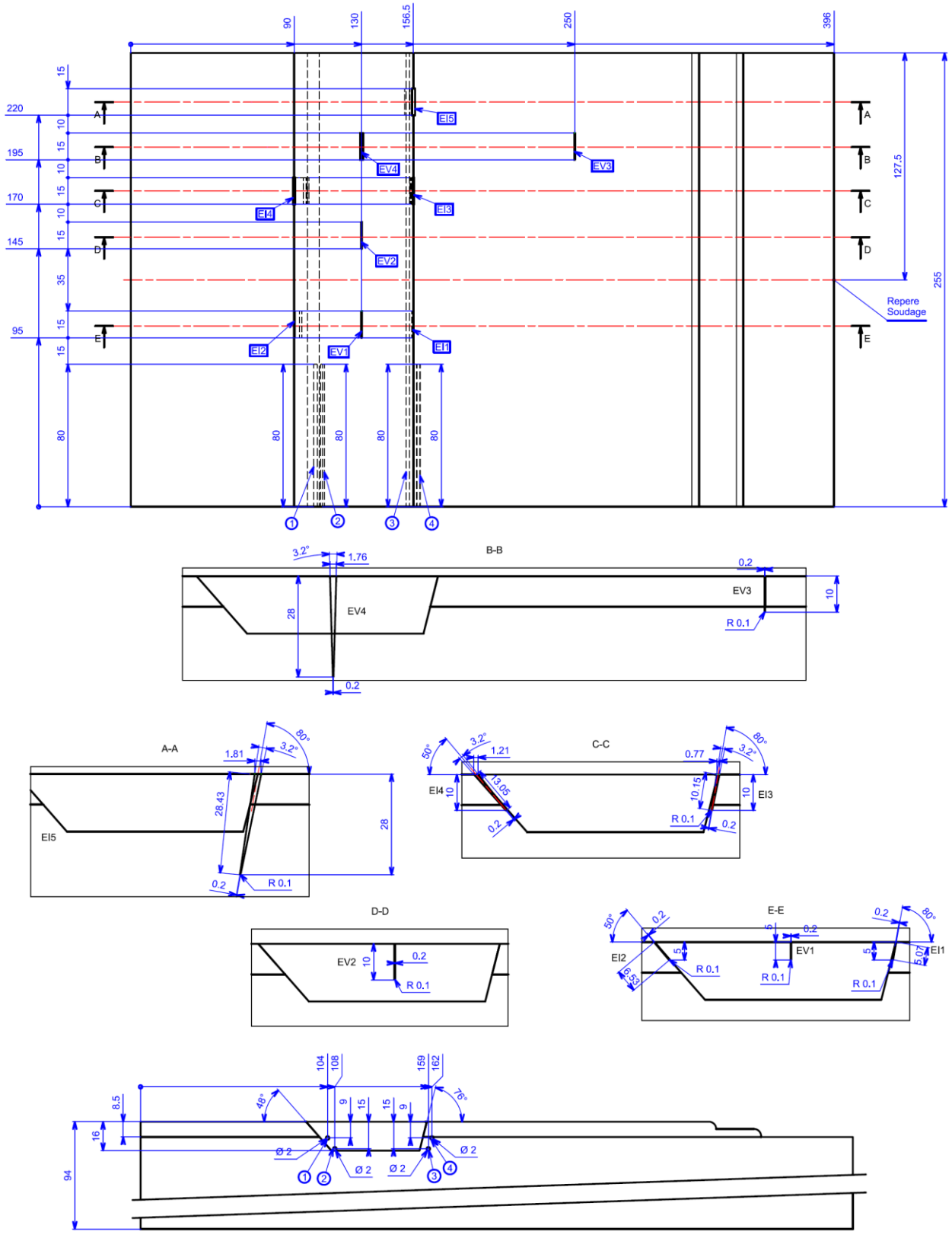

Figure 8.4: The sketch of the mock-up 1774-T248A